

# Quadratic Enhancement in the Reliability of Collective Quantum Engines

Noufal Jaseem,<sup>1</sup> Sai Vinjanampathy,<sup>2,3</sup> and Victor Mukherjee<sup>1</sup>

<sup>1</sup>*Department of Physical Sciences, Indian Institute of Science Education and Research Berhampur, Berhampur 760010, India.*

<sup>2</sup>*Department of Physics, Indian Institute of Technology-Bombay, Powai, Mumbai 400076, India.*

<sup>3</sup>*Centre for Quantum Technologies, National University of Singapore,  
3 Science Drive 2, 117543 Singapore, Singapore.*

Reducing fluctuations in the output of thermal machines is an important goal in classical as well as quantum technologies. We show that collective effects in open quantum systems can be harnessed to develop highly consistent many-body quantum machines. We consider quantum Otto engines, modeled by  $n$  spins collectively coupled to thermal baths. Our results show that collective effects can significantly reduce the fluctuations in the output work, quantified by high reliability ( $r$ ) and low thermodynamic uncertainty. In contrast to independent engines, we demonstrate a quadratic enhancement of the reliability  $r$  for their collective counterparts. This puts forward the case for realistic collective quantum thermal machines.

*Introduction.*— Modeling and control of quantum systems are crucial for the development of quantum technologies that exhibit an advantage over their classical analogs [1–7] such as computing, sensors and quantum thermal machines [1–19]. Each of these technologies is assessed by a performance benchmark, for instance, gate complexity for computing [20, 21] and variance of an unbiased estimator for sensors [11–19]. The performance of quantum thermal machines, on the other hand, has been evaluated through three key indicators, namely average efficiency, average output power, and more recently reliability ( $r$ ), quantified through the ratio of the average work to its root-mean-square deviation [22]. In this regard, various avenues relating to quantum correlations in small quantum systems, such as non-markovianity [23–27], optimizing paths [28–32] and exploiting non-thermal baths [33, 34] have been shown to enhance the performance of quantum machines. Following such theoretical investigations, several experimental realizations [35–39] of microscopic thermal machines have led to significant advancements in the fields of quantum thermodynamics and quantum technologies.

Many-body quantum systems offer unique opportunities to engineer quantum technologies operating in presence of non-trivial many-body effects, such as phase transitions [40–42], localization-delocalization transitions [43, 44] and cooperative effects arising due to collective interactions with environment [45]. Interestingly, collective effects have been shown to be highly beneficial in many quantum technologies [46–50], and have been used to enhance efficiency [51] and work output [45, 48, 52] in quantum heat engines, and perform high-precision quantum thermometry [48]. What remains an open question is if quantum correlations arising due to the environment can improve the consistency of quantum thermal machines. In this manuscript, we answer this crucial question in the affirmative and show that cooperative quantum effects can stabilize normalized fluctuations of a many-body engine better than their non-cooperative analogs. In general, reliability  $r$  in machines composed

of  $n$  subsystems scales as  $\sqrt{n}$  [53]. This leads to increased fluctuations in the microscopic regime, in machines comprising of a finite number of particles. In contrast, here we show that collective effects can result in the reliability  $r$  scaling as  $n$ , thus making collective quantum heat engines highly reliable, and paving a possible way for developing realistic and reliable quantum technologies. We begin by reviewing a generic model of a quantum engine and discuss the metrics for quantifying the performance of such an engine. For a quantum engine based on a generic many-body working medium (WM), we show that a broad class of steady-states results in a  $r \sim n$  scaling of the reliability, thus emphasizing the wide applicability of our results. We then exemplify our generic theory using specific examples of non-interacting as well as interacting multi-spin WMs. Finally, we summarize our main results.

*Reliable Collective Quantum Thermal Machines.*—

The performance of quantum thermal machines is assessed based on a variety of performance measures that examine the quality, quantity, and time in which a thermodynamic task is performed. In the case of quantum engines, two well-known metrics are output work and the efficiency of the engine. The third metric of performance is reliability, which measures the quality of output work considering it to be a fluctuating quantity. Reliability is defined as  $r = \langle W \rangle / \Delta W$ , where  $\langle W^p \rangle := \int_{-\infty}^{\infty} dW P(W) W^p$  is the moment of the work distribution function and  $\Delta W := \sqrt{\langle W^2 \rangle - \langle W \rangle^2}$  is the standard deviation. Reliability hence measures the consistency of the output work. Reliability has been investigated in a series of studies [54–61]. For instance, in [54] the impacts of diagnostic schemes to determine the performance of a quantum Otto heat engines on different figures of merit such as reliability are explored. In [55], a two-qudit swap engine is studied and it is shown that for fermionic swap engines the reliability is bound by  $r^2 \leq \langle \Sigma \rangle / (2 - \langle \Sigma \rangle)$ , where  $\langle \Sigma \rangle$  is the entropy production. The bosonic swap engines, on other hand, obeys  $r^2 \leq \langle \Sigma \rangle / (2 + \langle \Sigma \rangle)$  [56].

The different moments of the work distribution function are related to each other via the fluctuation-dissipation theorem, which can be formalised in terms of a thermodynamic uncertainty relation (TUR) [55, 56, 61–63]. A natural question that arises is whether the reliability of the engine can be enhanced by collective interactions. Consider  $n$  non-interacting quantum thermal machines. It is easy to see that the work and variance scale extensively with the size of the system [53]. This implies that the reliability scales as  $\mathcal{O}(\sqrt{n})$  which can be understood as the lower bound imposed by non-interacting systems [53]. In contrast, here we consider a generic many-body quantum engine collectively coupled to thermal baths, as depicted in Fig. 1, operating near the Carnot efficiency,  $\eta_C$ . It was previously established that for non-interacting collective quantum heat engines the mean output work scales as the collective heat capacity  $C^{\text{col}}$  in this case [48], see Appendix A. In this manuscript, we establish for a more generic setup that the variance of the output work also scales with  $C^{\text{col}}$ , which implies that so does  $r^2$ . Now, to understand the collective advantage in the reliability, let the generic non-equilibrium steady state of a  $n$ -body quantum engine operating near Carnot efficiency be written as  $\rho(\beta) = \exp(-\beta n \mathcal{A}) / \text{tr}[\exp(-\beta n \mathcal{A})]$  where  $\beta$  is the inverse temperature of a bath and  $\mathcal{A}$  is an operator in the collective basis which does not scale with system size. In this case, as we show below for appropriate  $\mathcal{A}$ ,  $C^{\text{col}} \propto n^2$  and hence the reliability scales as  $n$  (see Appendix B for details). This is a quadratic enhancement in the reliability of generic collective quantum thermal machines. We now demonstrate that our ansatz comes true for a many-body quantum Otto engine interacting collectively with a bath. Furthermore, owing to the scaling analysis, this ansatz can be chosen as a suitable design target for many-body quantum thermal machines.

*Many Body Otto Engine & Statistics.* — To illustrate and formalize our general result, we consider an Otto cycle of a many-body collective heat engine. The Otto cycle, described in Fig. 1 consists of four strokes namely: (i) (**A**  $\rightarrow$  **B**): We assume the WM starts from the steady state with respect to a thermal bath at temperature  $T_c$ . The frequency  $\omega$  of the WM is increased from  $\omega = \omega_c$  to  $\omega = \omega_h > \omega_c$  during this unitary stroke, thereby performing  $W_1$  amount of work on the system. (ii) (**B**  $\rightarrow$  **C**): The WM is coupled to a hot thermal bath during this non-unitary stroke, while the frequency is kept constant at  $\omega = \omega_h$ ;  $Q_h$  amount of heat flows from the hot bath to the WM, such that the WM reaches the steady state at the end of this stroke. (iii) (**C**  $\rightarrow$  **D**): The WM is decoupled from the bath after which the frequency is decreased from  $\omega = \omega_h$  to  $\omega = \omega_c$  during this unitary stroke;  $W_2$  amount of work is performed by the WM and (iv) (**D**  $\rightarrow$  **A**): The WM is coupled to a cold thermal bath during this non-unitary stroke, while its frequency is kept constant at  $\omega = \omega_c$ ;  $Q_c$  amount of heat flows from

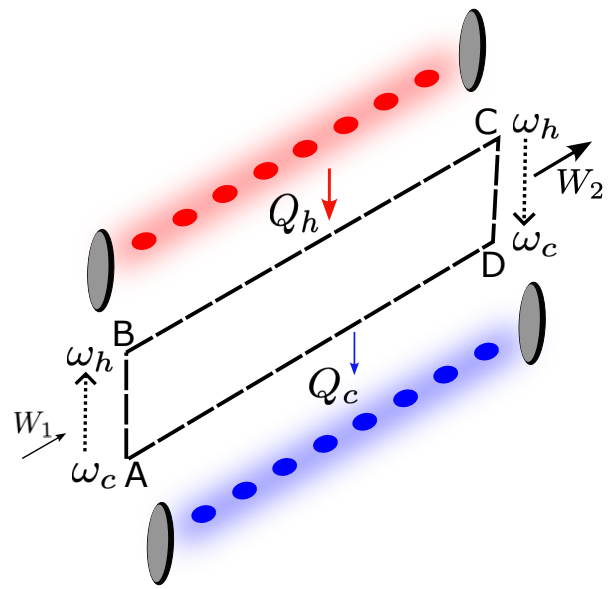


FIG. 1. We consider an Otto engine with a working medium consisting of an  $n$ -spin system interacting collectively with thermal baths as depicted schematically. Four strokes of the Otto cycle describe these collective bath interactions. Along paths AB and CD, the energy gap of the engine system is varied. Along paths BC and DA, the system interacts with collective baths as described in the text. The reliability of such an engine is shown in the text to have a quantum advantage.

the WM to the cold bath, such that the WM reaches the steady state at the end of this stroke, thereby completing the cycle.

The WM consists of multiple non-interacting identical spin  $s$  particles, described by the Hamiltonian  $H = \omega(t) \mathcal{J}_z$ . The collective angular momentum is defined as  $\mathcal{J}_i := \sum_{k=1}^n J_i^k$ , where  $J_i^k$  is the spin operator for the  $k$ th spin, along the direction  $i = x, y, z$ . The spins collectively exchange energy with the thermal baths during the non-unitary strokes through the interaction Hamiltonian  $H_{\text{int}} = \gamma \mathcal{J}_x \otimes \mathcal{B}_r$  ( $r = h, c$ ). Here  $\gamma$  denotes the interaction strength, while  $\mathcal{B}_c$  ( $\mathcal{B}_h$ ) is the bath operator for the cold (hot) bath. This collective system-bath interaction may result in non-zero off-diagonal terms in the steady-state density matrix  $\rho^{\text{ss}}$  of the WM at the end of non-unitary strokes in the local spin basis, signifying non-trivial steady-state quantum coherence in the many-body system. The dynamics of the WM are described by the master equation [45, 48, 64],

$$\frac{d\rho}{dt} = -i[H, \rho] + \alpha_c \mathcal{L}_c \rho + \alpha_h \mathcal{L}_h \rho. \quad (1)$$

Here,  $\mathcal{L}_{c(h)} \rho = \Gamma_{c(h)}(\omega_{c(h)}) \mathcal{D}(\mathcal{J}^+) \rho + \Gamma(-\omega_{c(h)}) \mathcal{D}(\mathcal{J}^-) \rho$ ,  $\mathcal{D}[O] \rho = (2O^\dagger \rho O - O O^\dagger \rho - \rho O O^\dagger) / 2$ ,  $\mathcal{J}^\pm := \mathcal{J}_x \pm i \mathcal{J}_y$  are the collective ladder operators of the spin system and  $\Gamma_c(\nu)$  ( $\Gamma_h(\nu)$ ) denotes the spectral function of the cold (hot) bath at frequency  $\nu$ , where we have consid-

ered the Kubo-Martin-Schwinger condition  $\Gamma_r(-\nu) = \exp(-\beta_r H) \Gamma_r(\nu)$  [23]. We have taken the physical constants  $\hbar = k_B = 1$ . The constant  $\alpha_{c(h)}$  is set to one if the system is coupled to the respective thermal bath, else it is zero.

We consider the system to interact collectively with the baths, such that the system steady states at **A** and **C** for the aforementioned dissipators (cf. Eq. (1)) can be written in the collective basis  $|j, m\rangle_i$  as [64]

$$\begin{aligned} \rho^{ss}(\beta, \omega) &= \sum_{j=j_0}^{ns} \sum_{i=1}^{l_j} P_{j,i} \rho_{j,i}^{\text{th}}(\beta, \omega), \\ \rho_{j,i}^{\text{th}}(\beta, \omega) &= \frac{1}{Z_j} \sum_{m=-j}^j e^{-\beta m \omega} |j, m\rangle_i \langle j, m|, \end{aligned} \quad (2)$$

with  $Z_j = \sum_{m=-j}^j e^{-\beta m \omega}$ . Here  $|j, m\rangle_i$  are the common eigenvectors of  $\mathcal{J}_z$  and  $\mathcal{J}^2 = \mathcal{J}_x^2 + \mathcal{J}_y^2 + \mathcal{J}_z^2$ ;  $-j \leq m \leq j$ ,  $j \in [j_0; ns]$ , and  $j_0 = 0$  for  $s \geq 1$ , while for  $s = 1/2$ , we have  $j_0 = 1/2$  for  $n$  odd and  $j_0 = 0$  for  $n$  even. The index  $i \in [1; l_j]$ , where  $l_j$  denotes the multiplicity of the eigenspaces associated to the eigenvalue  $j(j+1)$  of  $\mathcal{J}^2$  operator.  $P_{j,i} = \sum_{m=-j}^j \langle j, m | \rho_0 | j, m \rangle_i$ ,  $\rho_0$  being the initial state of the WM.

The dependence of  $\rho^{ss}$  on the initial state through  $P_{j,i}$  (cf. Eq. (2)) implies that a choice of  $P_{j,i}$  can influence the steady-state significantly. We have  $l_{j=ns} = 1$ , such that for  $P_{j=ns} = 1$  the steady state becomes

$$\rho^{ss}(\beta, \omega) = \sum_{m=-ns}^{ns} \frac{e^{-\beta m \omega}}{Z_{ns}} |ns, m\rangle \langle ns, m|, \quad (3)$$

which is a diagonal state in the symmetrical Dicke subspace known to produce a collective advantage [48]. This is in contrast with independent coupling between the particles of the WM and the bath, in which each spin thermalizes independently, such that the WM approaches a direct product steady state at the end of a non-unitary stroke [23, 45, 48, 64].

*Statistics of the many-body quantum heat engine.*—

Since heat and work are fluctuating quantities, a probability distribution maybe associated with obtaining a certain work  $W_1$  as  $P(W_1) = \sum_{m,n} \delta(W_1 + \epsilon_n^0 - \epsilon_m^\tau) p_{n \rightarrow m}^\tau p_n^0(\beta_c)$  [65]. Here,  $\epsilon_n^0$  and  $\epsilon_m^\tau$  are the respective energy eigenvalues corresponding to the collective energy eigenvectors which span the steady state at the beginning (time  $t = 0$ ) and at the end of the unitary stroke **A**  $\rightarrow$  **B** ( $t = \tau$ ) and  $p_n^0(\beta_c) = e^{-\beta_c \epsilon_n^0} / z_0$  is the initial occupation probability. The partition function is  $z_0 = \sum_l e^{-\beta_c \epsilon_l^0}$  and the transition probability during the adiabatic expansion is given by  $p_{n \rightarrow m}^\tau = |\langle n | U_{AB} | m \rangle|^2 = \delta_{n,m}$ . The unitary strokes are represented by the time-evolution operators  $U_{AB}$  or  $U_{CD}$ .

The conditional heat distribution of  $Q_h$  given the work  $W_1$  can be obtained as  $P(Q_h | W_1) = \sum_{k,l} \delta(Q_h + \epsilon_k^\tau -$

$\epsilon_l^\tau) p_{k \rightarrow l}^{\tau_2} p_k^\tau$  with occupation probability  $p_k^\tau = \delta_{km}$ . At the end of the non-unitary stroke, the state of the system is in a state in the symmetric subspace given by the Eq. (3) implying  $p_{k \rightarrow l}^{\tau_2} = p_l^{\tau_2}(\beta_h) = e^{-\beta_h \epsilon_l^\tau} / z_\tau$  with the partition function  $z_\tau = \sum_l e^{-\beta_h \epsilon_l^\tau}$ . Furthermore, we have the conditional quantum work distribution for compression given the expansion work  $W_1$  and the heat  $Q_h$  as  $P(W_2 | Q_h, W_1) = \sum_{i,j} \delta(W_2 + \epsilon_i^\tau - \epsilon_j^0) p_{i \rightarrow j}^\tau p_i^{\tau+\tau_2}$ . The transition probability  $p_{i \rightarrow j}^\tau = |\langle i | U_{CD} | j \rangle|^2 = \delta_{ij}$  selects for adiabatic transformations and likewise  $p_i^{\tau+\tau_2} = \delta_{il}$  implies that we start with state  $|ns, l\rangle$  in the step that extracts  $W_2$ . The joint probability  $P(W, Q_h)$  of having certain values of net work  $W = W_2 + W_1$  and heat  $Q_h$  during one cycle of the Otto engine can be readily calculated using the chain rule for conditional probabilities (see Appendix C). The associated characteristic function  $\chi(\gamma_1, \gamma_2)$  is given by

$$\chi(\gamma_1, \gamma_2) = \iint_{-\infty}^{\infty} dW dQ_h e^{i\gamma_1 W} e^{i\gamma_2 Q_h} P(W, Q_h), \quad (4)$$

which can then be used to compute the various moments of the heat and work distribution function as

$$\langle W^r Q_h^s \rangle = \frac{\partial^r}{\partial (i\gamma_1)^r} \frac{\partial^s}{\partial (i\gamma_2)^s} \chi(\gamma_1, \gamma_2) \Big|_{\gamma_{1,2}=0}. \quad (5)$$

*n qubit collective engine.*— Next for simplicity we focus on  $s = 1/2$  (see Appendix C for generic  $s$ )  $n$  qubit engine with system Hamiltonian  $H = \omega(t) \sum_{i=1}^n \sigma_z^i$ , which interacts collectively with the thermal baths. We consider the regime close to the Carnot efficiency bound, where the work output approaches zero and hence where work fluctuations can be expected to be prominent. To quantify the reliability advantage of a collective quantum heat engine, we define the ratio of reliability of the collective engine to that of the independent engine:  $\lambda_r = r_{\text{col}}^2 / r_{\text{ind}}^2$ . In the limit  $T_h \rightarrow \infty$  and  $\eta = -\langle W \rangle / Q_h \rightarrow \eta_C = 1 - T_c / T_h$ , one can verify that  $\text{var}(W_{\text{col}}) \propto C^{\text{col}} \sim n^2$  (see Appendix D). A value of  $\lambda_r > 1$  implies lower relative noise to signal ratio for the collective quantum heat engine (QHE), as compared to the independent one, signifying higher consistency in the output of collective QHEs. The parameter  $\lambda_r$  close to the Carnot bound is plotted in Fig. 2. The remarkable advantage offered by the collective effects is shown by large values of  $\lambda_r$  in Fig. 2, specially in the limit of large  $n$  and  $T_h$ . Clearly, high temperature  $T_h$  of the hot bath and large system size  $n$  allow operation of the collective QHE with high reliability in the work output. Interestingly, this regime is also the most beneficial for high mean work output  $\langle W_{\text{col}} \rangle \sim n^2$ , as discussed in Refs. [45] and [48]. Further,  $\lambda_r$  increases linearly with  $n$  for  $\beta_h \rightarrow 0$ , implying consistency of collective engines increases extensively with system size. Interestingly, quadratic advantage in reliability can be obtained for more general Hamiltonian with inter-particle interactions as well, such as  $H = n\omega(t)(\mathcal{J}_z/n)^x$  for  $x > 1$ ; the collective advantage persists if the steady state is restricted to the

$j = ns$  subspace, and is of the general form  $\rho^{ss}(\beta, \omega) = \sum_{m=-ns}^{ns} \exp[-\beta n(m/n)x\omega] / Z_{ns}^{(x)} |ns, m\rangle \langle ns, m|$ ,  $Z_{ns}^{(x)} = \sum_{m=-ns}^{ns} \exp[-\beta n(m/n)x\omega]$ . The heat capacity for such interacting systems is derived in Appendix B.

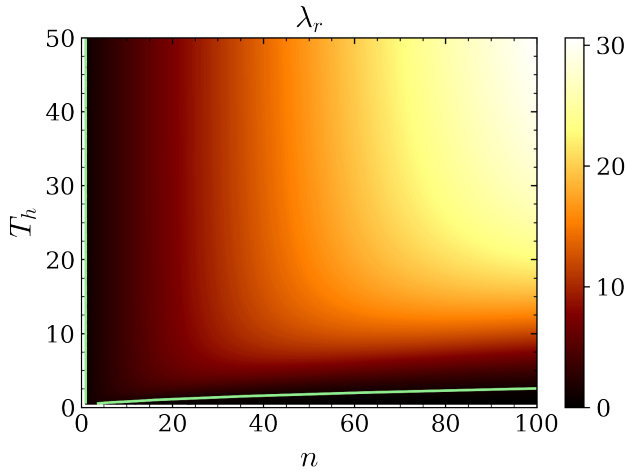


FIG. 2. The ratio of reliability of collective engine to that of the independent engine,  $\lambda_r$ , is plotted against  $n$  and  $T_h$ , for efficiency close to the Carnot bound. The advantage of collective QHEs over independent ones become more pronounced for large  $T_h$  and  $n$ . The green line is the contour line for  $\lambda_r = 1$ . Parameter values are  $\omega_h = 0.5$ ,  $\omega_c = 0.1$ , and  $\Delta = \beta_c \omega_c - \beta_h \omega_h = 0.01$ .

*Entropy Production & TUR.*— Having demonstrated the collective advantage in the reliability of a many-body correlated heat engine, we turn to the issue of entropy production. It is desirable to have an engine with low entropy production to enhance efficiency. However, it is known that the entropy production and the reliability are not independent of each other and there exists a lower bound for the product of entropy production and the inverse of the square of the reliability [54, 55, 57–61]. For our collective engine, we can show that the enhanced reliability does not come at the cost of large entropy production. In other words, their product can be made smaller than the standard TUR bound. The efficiency  $\eta$  of an engine is related to the entropy production  $\langle \Sigma \rangle$  through the relation:

$$\langle \Sigma \rangle = -\frac{\langle Q_h \rangle}{T_h} - \frac{\langle Q_c \rangle}{T_c} = \frac{\langle W \rangle}{T_c} \left( \frac{\eta_c}{\eta} - 1 \right). \quad (6)$$

For the collective heat engine, the desired low fluctuating output work is obtained at a thermodynamic cost of an increased entropy production  $\langle \Sigma \rangle$ , following the inequality in the large  $n$ -limit [55]:

$$\left( \frac{1}{r_{col}} \right)^2 = \frac{f(\{\beta_i \omega_i\})}{\langle \Sigma_{col} \rangle} - 1 \geq \frac{2}{\langle \Sigma_{col} \rangle} - 1. \quad (7)$$

where  $f(\{\beta_i \omega_i\}) = (\beta_c \omega_c - \beta_h \omega_h)(a/b) \geq 2$  (see Appendix E),  $a = \cosh(\beta_c \omega_c - \beta_h \omega_h) + \cosh \beta_c \omega_c + \cosh \beta_h \omega_h - 3$  and

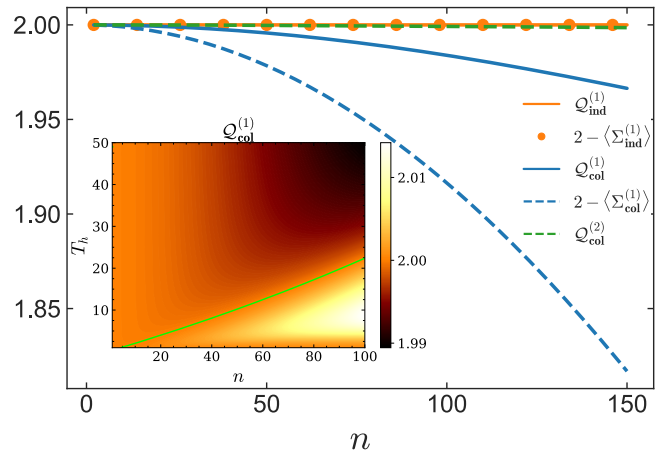


FIG. 3. The left and right-hand sides of the TUR, in Eq.(8), are plotted as a function of the number of spins  $n$  for the collective and independent cases. Superscripts of  $Q$  and  $\Sigma$  are for  $x = 1, 2$ . Parameter values are set as  $\omega_h = 0.5$ ,  $\omega_c = 0.1$ ,  $\beta_h \rightarrow 0$  and  $\Delta = \beta_c \omega_c - \beta_h \omega_h = 0.01$ . Inset:  $Q_{col}^{(1)}$  is plotted as a function of the temperature of the hot bath  $T_h$  and the number of spins  $n$ . Low  $Q_{col}^{(1)}$  for large  $T_h$  and  $n$  implies the collective engine is most beneficial in this regime. The green line is the contour line for  $Q_{col}^{(1)} = 2$ . Parameter values are the same as above except  $T_h$  whose value is varied along the  $y$  axis.

$b = \sinh(\beta_c \omega_c - \beta_h \omega_h) - \sinh \beta_c \omega_c + \sinh \beta_h \omega_h$ . Consequently, one can arrive at a trade-off, quantified by the thermodynamic uncertainty  $Q = \langle \Sigma \rangle / r^2$  [61, 63]. For a classical system  $Q \geq 2$ , this is known as the standard TUR which provides a lower bound for  $Q$ . For the  $n$ -qubit collective Otto engine, this is given by

$$Q \geq 2 - \langle \Sigma \rangle, \quad (8)$$

which further sharpens the TUR in the quantum case. Since the entropy production  $\langle \Sigma_{col} \rangle \geq 0$ , the collective engine TUR  $Q_{col} \geq 2 - \langle \Sigma_{col} \rangle$  may violate the standard TUR bound, implying once again, a collective effect induced improvement in performance. Recently such violations have been observed for quantum-coherent and quantum-entangled systems [55, 57–61]. In Fig. 3 the uncertainty  $Q$  as well as its lower bound are plotted for the collective and independent cases. The figure inset shows that in the large  $n$  and  $T_h$  limit, the  $Q < 2$ ; this is the region where the collective effects lead to a maximal advantage over the independent case as shown in Fig. 2.

*Discussion.*— In this manuscript, we have considered QHEs modeled by generic many-body quantum systems collectively coupled to thermal baths. We have shown that for a broad class of steady states arising due to collective system-bath coupling, one can get a quadratic advantage in reliability, as compared to their independent counterparts. We have then explicitly shown this collective advantage in reliability for collective QHEs with non-interacting as well as interacting multi-spin WMs.

Interestingly, this collective advantage increases with increasing temperature  $T_h$  of the hot bath as well as size  $n$  of the working medium. We also studied TUR in such collective QHEs; the advantage due to collective effects persists in this case as well, in form of low thermodynamic uncertainty and TUR bound, as compared to the independent QHEs, for high  $T_h$ . Furthermore,  $Q_{col} < 2$  for high  $T_h$  and large  $n$ , thereby violating the standard TUR bound in these regimes.

Several existing platforms can be expected to be ideal for experimentally realizing such collective QHEs. For example, experimental realization of collective effects is well established in cavity systems, such as by using Rydberg atoms in a cavity [66]; recently, collective effect in the form of superabsorption in an organic microcavity has been used to charge a quantum battery [67]. The collective phenomenon of superradiance has been observed in atomic sodium [68] as well as in quantum dots [69]. Recent advancements in techniques to assemble atoms with great control using optical tweezers [70–74], and optical lattices [75–78] is also a promising development that can be used to design desired many-body quantum systems.

Miniaturization of machines is one of the major aims of research in science and technology. However, this is associated with the challenge of fluctuations increasing with decreasing system size [53]. In that context, the collective QHEs studied in this manuscript can be highly beneficial, owing to their high reliability and low thermodynamic uncertainty ratio  $Q_{col}$ . The results presented in this manuscript show conclusively the remarkable advantage offered by collective effects in designing highly reliable many-body quantum thermal machines, thereby paving a path to realizing highly reliable mesoscopic quantum thermal machines.

## ACKNOWLEDGEMENTS

V.M. acknowledges support from Science and Engineering Research Board (SERB) through MATRICS (Project No. MTR/2021/000055) and Seed Grant from IISER Berhampur. S.V. acknowledges support from the Government of India DST-QUEST grant number DST/ICPS/QuST/Theme-4/2019.

---

[1] Ronnie Kosloff and Amikam Levy. Quantum heat engines and refrigerators: Continuous devices. *Annual Review of Physical Chemistry*, 65(1):365–393, 2014. PMID: 24689798.

[2] David Gelbwaser-Klimovsky, Wolfgang Niedenzu, and Gershon Kurizki. Chapter twelve - thermodynamics of quantum systems under dynamical control. volume 64 of *Advances In Atomic, Molecular, and Optical Physics*, pages 329–407. Academic Press, 2015.

[3] Sai Vinjanampathy and Janet Anders. Quantum thermodynamics. *Contemporary Physics*, 57(4):545–579, 2016.

[4] John Goold, Marcus Huber, Arnau Riera, Lidia del Rio, and Paul Skrzypczyk. The role of quantum information in thermodynamics—a topical review. *Journal of Physics A: Mathematical and Theoretical*, 49(14):143001, Feb 2016.

[5] Sourav Bhattacharjee and Amit Dutta. Quantum thermal machines and batteries. *The European Physical Journal B*, 94(12):239, Dec 2021.

[6] Victor Mukherjee and Uma Divakaran. Many-body quantum thermal machines. *Journal of Physics: Condensed Matter*, 33(45):454001, Aug 2021.

[7] Nathan M. Myers, Obinna Abah, and Sebastian Deffner. Quantum thermodynamic devices: From theoretical proposals to experimental reality. *AVS Quantum Science*, 4(2):027101, 2022.

[8] Robert Raussendorf and Hans J. Briegel. A one-way quantum computer. *Phys. Rev. Lett.*, 86:5188–5191, May 2001.

[9] David Kielpinski, Chris Monroe, and David J Wineland. Architecture for a large-scale ion-trap quantum computer. *Nature*, 417(6890):709–711, 2002.

[10] C Monroe, R Raussendorf, A Ruthven, KR Brown, P Maunz, L-M Duan, and J Kim. Large-scale modular quantum-computer architecture with atomic memory and photonic interconnects. *Physical Review A*, 89(2):022317, 2014.

[11] D. J. Wineland, J. J. Bollinger, W. M. Itano, F. L. Moore, and D. J. Heinzen. Spin squeezing and reduced quantum noise in spectroscopy. *Phys. Rev. A*, 46:R6797–R6800, Dec 1992.

[12] Vittorio Giovannetti, Seth Lloyd, and Lorenzo Maccone. Quantum-enhanced measurements: beating the standard quantum limit. *Science*, 306(5700):1330–1336, 2004.

[13] Bernard Yurke, Samuel L. McCall, and John R. Klauder.  $Su(2)$  and  $su(1,1)$  interferometers. *Phys. Rev. A*, 33:4033–4054, Jun 1986.

[14] Jonathan P. Dowling. Correlated input-port, matter-wave interferometer: Quantum-noise limits to the atom-laser gyroscope. *Phys. Rev. A*, 57:4736–4746, Jun 1998.

[15] J. J. Bollinger, Wayne M. Itano, D. J. Wineland, and D. J. Heinzen. Optimal frequency measurements with maximally correlated states. *Phys. Rev. A*, 54:R4649–R4652, Dec 1996.

[16] R Demkowicz-Dobrzanski, M Jarzyna, and J Kolodynski. Chapter four-quantum limits in optical interferometry, volume 60 of. *Progress in Optics*, pages 345–435.

[17] Jonathan P Dowling. Quantum optical metrology—the lowdown on high-n00n states. *Contemporary physics*, 49(2):125–143, 2008.

[18] Noufal Jaseem, S Omkar, and Anil Shaji. Quantum critical environment assisted quantum magnetometer. *Journal of Physics A: Mathematical and Theoretical*, 51(17):175309, 2018.

[19] Noufal Jaseem and Anil Shaji. Two-mode gaussian product states in a lossy interferometer. *Quantum Information Processing*, 16(9):1–14, 2017.

[20] Tatsuhiko Koike and Yosuke Okudaira. Time complexity and gate complexity. *Phys. Rev. A*, 82:042305, Oct 2010.

[21] Srinivas Sridharan, Mile Gu, Matthew R. James, and William M. McEneaney. Reduced-complexity numerical method for optimal gate synthesis. *Phys. Rev. A*, 82:042319, Oct 2010.

- [22] Massimiliano Esposito, Upendra Harbola, and Shaul Mukamel. Nonequilibrium fluctuations, fluctuation theorems, and counting statistics in quantum systems. *Rev. Mod. Phys.*, 81:1665–1702, Dec 2009.
- [23] H. P. Breuer and F. Petruccione. *The Theory of Open Quantum Systems*. Oxford University Press, 2002.
- [24] Victor Mukherjee, Abraham G. Kofman, and Gershon Kurizki. Anti-zeno quantum advantage in fast-driven heat machines. *Communications Physics*, 3(1):8, Jan 2020.
- [25] Arpan Das and Victor Mukherjee. Quantum-enhanced finite-time otto cycle. *Phys. Rev. Research*, 2:033083, Jul 2020.
- [26] Michael Wiedmann, Jürgen T. Stockburger, and Joachim Ankerhold. Non-markovian quantum otto refrigerator. *The European Physical Journal Special Topics*, 230(4):851–857, Jun 2021.
- [27] Sai Vinjanampathy and Kavan Modi. Correlations, operations and the second law of thermodynamics. *International Journal of Quantum Information*, 14(06):1640033, 2016.
- [28] Nishchay Suri, Felix C Binder, Bhaskaran Muralidharan, and Sai Vinjanampathy. Speeding up thermalisation via open quantum system variational optimisation. *The European Physical Journal Special Topics*, 227(3):203–216, 2018.
- [29] P A Erdman, V Cavina, R Fazio, F Taddei, and V Giovannetti. Maximum power and corresponding efficiency for two-level heat engines and refrigerators: optimality of fast cycles. *New Journal of Physics*, 21(10):103049, Oct 2019.
- [30] Vasco Cavina, Paolo A. Erdman, Paolo Abiuso, Leonardo Tolomeo, and Vittorio Giovannetti. Maximum-power heat engines and refrigerators in the fast-driving regime. *Phys. Rev. A*, 104:032226, Sep 2021.
- [31] Paolo A. Erdman and Frank Noé. Identifying optimal cycles in quantum thermal machines with reinforcement-learning. *npj Quantum Information*, 8(1):1, Jan 2022.
- [32] Iliia Khait, Juan Carrasquilla, and Dvira Segal. Optimal control of quantum thermal machines using machine learning. *Phys. Rev. Research*, 4:L012029, Mar 2022.
- [33] J. Roßnagel, O. Abah, F. Schmidt-Kaler, K. Singer, and E. Lutz. Nanoscale heat engine beyond the carnot limit. *Phys. Rev. Lett.*, 112:030602, Jan 2014.
- [34] Wolfgang Niedenzu, Victor Mukherjee, Arnab Ghosh, Abraham G. Kofman, and Gershon Kurizki. Quantum engine efficiency bound beyond the second law of thermodynamics. *Nature Communications*, 9(1):165, Jan 2018.
- [35] Johannes Roßnagel, Samuel T. Dawkins, Karl N. Tolazzi, Obinna Abah, Eric Lutz, Ferdinand Schmidt-Kaler, and Kilian Singer. A single-atom heat engine. *Science*, 352(6283):325–329, 2016.
- [36] Jan Klaers, Stefan Faelt, Atac Imamoglu, and Emre Togan. Squeezed thermal reservoirs as a resource for a nanomechanical engine beyond the carnot limit. *Phys. Rev. X*, 7:031044, Sep 2017.
- [37] Gleb Maslennikov, Shiqian Ding, Roland Hablützel, Jaren Gan, Alexandre Roulet, Stefan Nimmrichter, Jibo Dai, Valerio Scarani, and Dzmitry Matsukevich. Quantum absorption refrigerator with trapped ions. *Nature Communications*, 10(1):202, Jan 2019.
- [38] James Klatzow, Jonas N. Becker, Patrick M. Ledingham, Christian Weinzetl, Krzysztof T. Kaczmarek, Dylan J. Saunders, Joshua Nunn, Ian A. Walmsley, Raam Uzdin, and Eilon Poem. Experimental demonstration of quantum effects in the operation of microscopic heat engines. *Phys. Rev. Lett.*, 122:110601, Mar 2019.
- [39] Soham Pal, Sushant Saryal, Dvira Segal, T. S. Mahesh, and Bijay Kumar Agarwalla. Experimental study of the thermodynamic uncertainty relation. *Phys. Rev. Research*, 2:022044, May 2020.
- [40] Michele Campisi and Rosario Fazio. The power of a critical heat engine. *Nature Communications*, 7(1):11895, Jun 2016.
- [41] Revathy B. S, Victor Mukherjee, Uma Divakaran, and Adolfo del Campo. Universal finite-time thermodynamics of many-body quantum machines from kibble-zurek scaling. *Phys. Rev. Research*, 2:043247, Nov 2020.
- [42] Thomás Fogarty and Thomas Busch. A many-body heat engine at criticality. *Quantum Science and Technology*, 6(1):015003, Nov 2020.
- [43] Nicole Yunger Halpern, Christopher David White, Sarang Gopalakrishnan, and Gil Refael. Quantum engine based on many-body localization. *Phys. Rev. B*, 99:024203, Jan 2019.
- [44] Cecilia Chiaracane, Mark T. Mitchison, Archak Purkayastha, Géraldine Haack, and John Goold. Quasiperiodic quantum heat engines with a mobility edge. *Phys. Rev. Research*, 2:013093, Jan 2020.
- [45] Wolfgang Niedenzu and Gershon Kurizki. Cooperative many-body enhancement of quantum thermal machine power. *New Journal of Physics*, 20(11):113038, Nov 2018.
- [46] Carlos A Perez-Delgado and Sai Vinjanampathy. Coherent parallelization of universal classical computation. *New Journal of Physics*, 23(12):123015, 2021.
- [47] Angsar Manatuly, Wolfgang Niedenzu, Ricardo Román-Ancheyta, Barı̇ş Çakmak, Özgür E. Müstecaplıođlu, and Gershon Kurizki. Collectively enhanced thermalization via multiqubit collisions. *Phys. Rev. E*, 99:042145, Apr 2019.
- [48] C L Latune, I Sinayskiy, and F Petruccione. Collective heat capacity for quantum thermometry and quantum engine enhancements. *New Journal of Physics*, 22(8):083049, Aug 2020.
- [49] Gentaro Watanabe, B. Prasanna Venkatesh, Peter Talkner, Myung-Joong Hwang, and Adolfo del Campo. Quantum statistical enhancement of the collective performance of multiple bosonic engines. *Phys. Rev. Lett.*, 124:210603, May 2020.
- [50] Michal Hajdušek, Parvinder Solanki, Rosario Fazio, and Sai Vinjanampathy. Seeding crystallization in time. *Physical Review Letters*, 128(8):080603, 2022.
- [51] David Gelbwaser-Klimovsky, Wassilij Kopylov, and Gernot Schaller. Cooperative efficiency boost for quantum heat engines. *Phys. Rev. A*, 99:022129, Feb 2019.
- [52] Michal Kloc, Pavel Cejnar, and Gernot Schaller. Collective performance of a finite-time quantum otto cycle. *Phys. Rev. E*, 100:042126, Oct 2019.
- [53] F. Reif. *Fundamentals of Statistical and Thermal Physics*. Waveland Press, Inc., 2009.
- [54] Jeongrak Son, Peter Talkner, and Juzar Thingna. Monitoring quantum otto engines. *PRX Quantum*, 2(4):040328, 2021.
- [55] Massimiliano F Sacchi. Multilevel quantum thermodynamic swap engines. *Physical Review A*, 104(1):012217, 2021.

- [56] Massimiliano F. Sacchi. Thermodynamic uncertainty relations for bosonic otto engines. *Phys. Rev. E*, 103:012111, Jan 2021.
- [57] Bijay Kumar Agarwalla and Dvira Segal. Assessing the validity of the thermodynamic uncertainty relation in quantum systems. *Physical Review B*, 98(15):155438, 2018.
- [58] Krzysztof Ptaszyński. Coherence-enhanced constancy of a quantum thermoelectric generator. *Physical Review B*, 98(8):085425, 2018.
- [59] Giacomo Guarnieri, Gabriel T Landi, Stephen R Clark, and John Goold. Thermodynamics of precision in quantum nonequilibrium steady states. *Physical Review Research*, 1(3):033021, 2019.
- [60] Loris Maria Cangemi, Vittorio Cataudella, Giuliano Benenti, Maura Sasseti, and Giulio De Filippis. Violation of thermodynamics uncertainty relations in a periodically driven work-to-work converter from weak to strong dissipation. *Physical Review B*, 102(16):165418, 2020.
- [61] Alex Arash Sand Kalae, Andreas Wacker, and Patrick P Potts. Violating the thermodynamic uncertainty relation in the three-level maser. *Physical Review E*, 104(1):L012103, 2021.
- [62] Kosuke Ito, Chao Jiang, and Gentaro Watanabe. Universal bounds for fluctuations in small heat engines. *arXiv preprint arXiv:1910.08096*, 2019.
- [63] Jordan M Horowitz and Todd R Gingrich. Thermodynamic uncertainty relations constrain non-equilibrium fluctuations. *Nature Physics*, 16(1):15–20, 2020.
- [64] Camille L Latune, Ilya Sinayskiy, and Francesco Petruccione. *Phys. Rev. Research*, 1:033192, 2019.
- [65] Tobias Denzler. *Fluctuations and correlations of quantum heat engines*. PhD thesis, University of Stuttgart, 2020.
- [66] J. M. Raimond, P. Goy, M. Gross, C. Fabre, and S. Haroche. Collective absorption of blackbody radiation by rydberg atoms in a cavity: An experiment on bose statistics and brownian motion. *Phys. Rev. Lett.*, 49:117–120, Jul 1982.
- [67] James Q Quach, Kirsty E McGhee, Lucia Ganzer, Dominic M Rouse, Brendon W Lovett, Erik M Gauger, Jonathan Keeling, Giulio Cerullo, David G Lidzey, and Tersilla Virgili. Superabsorption in an organic microcavity: Toward a quantum battery. *Science advances*, 8(2):eabk3160, 2022.
- [68] M Gross, C Fabre, P Pillet, and S Haroche. Observation of near-infrared dicke superradiance on cascading transitions in atomic sodium. *Physical Review Letters*, 36(17):1035, 1976.
- [69] Michael Scheibner, Thomas Schmidt, Lukas Worschech, Alfred Forchel, Gerd Bacher, Thorsten Passow, and Detlef Hommel. Superradiance of quantum dots. *Nature Physics*, 3(2):106–110, 2007.
- [70] Jun Rui, David Wei, Antonio Rubio-Abadal, Simon Hollerith, Johannes Zeiher, Dan M Stamper-Kurn, Christian Gross, and Immanuel Bloch. A subradiant optical mirror formed by a single structured atomic layer. *Nature*, 583(7816):369–374, 2020.
- [71] Daniel Ohl De Mello, Dominik Schäffner, Jan Werkmann, Tilman Preuschoff, Lars Kohfahl, Malte Schlosser, and Gerhard Birkel. Defect-free assembly of 2d clusters of more than 100 single-atom quantum systems. *Physical review letters*, 122(20):203601, 2019.
- [72] Antoine Glicenstein, Giovanni Ferioli, Nikola Šibalić, Ludovic Brossard, Igor Ferrier-Barbut, and Antoine Browaeys. Collective shift in resonant light scattering by a one-dimensional atomic chain. *Physical Review Letters*, 124(25):253602, 2020.
- [73] Daniel Barredo, Sylvain De Léséleuc, Vincent Lienhard, Thierry Lahaye, and Antoine Browaeys. An atom-by-atom assembler of defect-free arbitrary two-dimensional atomic arrays. *Science*, 354(6315):1021–1023, 2016.
- [74] Manuel Endres, Hannes Bernien, Alexander Keesling, Harry Levine, Eric R Anschuetz, Alexandre Krajenbrink, Crystal Senko, Vladan Vuletic, Markus Greiner, and Mikhail D Lukin. Atom-by-atom assembly of defect-free one-dimensional cold atom arrays. *Science*, 354(6315):1024–1027, 2016.
- [75] Aishwarya Kumar, Tsung-Yao Wu, Felipe Giraldo, and David S Weiss. Sorting ultracold atoms in a three-dimensional optical lattice in a realization of maxwell’s demon. *Nature*, 561(7721):83–87, 2018.
- [76] Daniel Greif, Maxwell F Parsons, Anton Mazurenko, Christie S Chiu, Sebastian Blatt, Florian Huber, Geoffrey Ji, and Markus Greiner. Site-resolved imaging of a fermionic mott insulator. *Science*, 351(6276):953–957, 2016.
- [77] Jacob F Sherson, Christof Weitenberg, Manuel Endres, Marc Cheneau, Immanuel Bloch, and Stefan Kuhr. Single-atom-resolved fluorescence imaging of an atomic mott insulator. *Nature*, 467(7311):68–72, 2010.
- [78] Waseem S Bakr, Amy Peng, M Eric Tai, Ruichao Ma, Jonathan Simon, Jonathon I Gillen, Simon Foelling, Lode Pollet, and Markus Greiner. Probing the superfluid-to-mott insulator transition at the single-atom level. *Science*, 329(5991):547–550, 2010.

## Appendix A: Work output of an Otto engine

The total work output of an Otto engine is the sum of the work done on the system and by the system during the adiabatic unitary strokes. That is,  $\langle W \rangle = \langle W_1 \rangle + \langle W_2 \rangle = \text{Tr}\{[H_h - H_c]\rho_c\} + \text{Tr}\{[H_c - H_h]\rho_h\} = (\omega_h - \omega_c)\text{Tr}\{\mathcal{J}_z[\rho_h - \rho_c]\}$ . We have used the following definitions and identities here and in the following derivations:  $H(\omega_k) = \frac{1}{2}\omega_k\mathcal{J}_z$ ,  $\rho_k = \rho^{ss}(\theta_k)$ ,  $\theta_{c(h)} = \beta_{c(h)}\omega_{c(h)}$ ,  $\Delta\eta = \eta_c - \eta = \frac{\theta_c - \theta_h}{\beta_c\omega_h}$ ,  $\eta_c$  is the Carnot efficiency, and  $\Delta\theta = \theta_c - \theta_h = \beta_c\omega_h\Delta\eta$ . Near the Carnot limit ( $\Delta\eta \approx 0$ ), the work can be written as  $\langle W \rangle = (\omega_c - \omega_h)\beta_c\omega_h\Delta\eta \frac{\partial}{\partial\theta}\text{Tr}\{\mathcal{J}_z\rho(\theta)\}|_{\theta_h} + O(\Delta\eta^2)$ .

One can show that,  $\frac{\partial}{\partial\theta}\text{Tr}\{\mathcal{J}_z\rho(\theta)\}|_{\theta_h} = -\frac{C(\theta_h)}{k_B\theta_h^2}$  for both independent and collective cases, where  $C$  is the heat capacity of the spin system. And also,  $\omega_c - \omega_h = (\beta_c\omega_h - \beta_h\omega_h - \beta_c\omega_h\Delta\eta)/\beta_c$ . Thus the average work is related to heat capacity as [48],  $\langle W \rangle = -\Delta\eta\omega_h^2(\beta_c - \beta_h) \frac{C(\theta_h)}{k_B\theta_h^2} + O(\Delta\eta^2)$ . For an  $n$  qubit system with inverse temperature  $\beta$ , the heat capacity is given by  $C_{col} = -k_B\beta^2 \frac{\partial}{\partial\beta}\text{Tr}(H\rho^{ss}) = \frac{1}{4}k_B\beta^2\omega^2 \left[ \text{csch}^2 \frac{\beta\omega}{2} - (n+1)^2 \text{csch}^2 \frac{(n+1)\beta\omega}{2} \right]$ . At large temperatures, the heat capacity reduces to  $C_{col} \approx \frac{1}{12}k_B\beta^2\omega^2 n(n+2)$ , hence we obtain,  $\langle W \rangle \propto n^2$ .

## Appendix B: $n^2$ scaling of work, its variance and heat capacity for $H = n\omega(\mathcal{J}_z/n)^x$

Let the Hamiltonian be  $H = n\omega(\mathcal{J}_z/n)^x$ , where  $\mathcal{J}_z = \sum_i \sigma_z^i$ . Following the steps given in the Appendices A and D, we can show that  $\langle W \rangle = -\Delta\eta\omega_h^2(\beta_c - \beta_h) \frac{C(\theta_h)}{k_B\theta_h^2} + O(\Delta\eta^2)$  and  $\text{var}(W) = (\omega_c - \omega_h)^2 \left\{ \frac{C(\theta_h)}{k_B\theta_h^2} + \frac{C(\theta_c)}{k_B\theta_c^2} \right\}$  for this case as well. Let the steady state be of the form  $\rho^{ss} = e^{-\beta\omega H}/z$  where  $z = \text{tr}(e^{-\beta\omega H})$ . Then heat capacity can be obtained using standard arguments as

$$A = \left[ e^{(2ns+1)(\theta_h + i\gamma_1\omega_h)} - e^{i(2ns+1)(\gamma_1\omega_c + \gamma_2\omega_h)} \right] \left[ e^{i(2ns+1)\gamma_1\omega_h} - e^{(2ns+1)[\theta_c + i(\gamma_1\omega_c + \gamma_2\omega_h)]} \right] \sinh \frac{\theta_c}{2} \text{csch} \frac{(2ns+1)\theta_c}{2}$$

$$\sinh \frac{\theta_h}{2} \text{csch} \frac{(2ns+1)\theta_h}{2} e^{-ns\{\theta_c + \theta_h + 2i[\gamma_1(\omega_c + \omega_h) + \gamma_2\omega_h]\}},$$

$$B = \left[ e^{i\gamma_1\omega_h} - e^{\theta_c + i(\gamma_1\omega_c + \gamma_2\omega_h)} \right] \left[ e^{(\theta_h + i\gamma_1\omega_h)} - e^{i(\gamma_1\omega_c + \gamma_2\omega_h)} \right], \quad \theta_{c(h)} = \beta_{c(h)}\omega_{c(h)}.$$

For  $s = 1/2$  n-qubit engine, the general spin  $s$  characteristic function simplifies to  $\chi = A_1/B_1$ , where,

$$A_1 = \sinh \frac{\theta_c}{2} \sinh \frac{\theta_h}{2} \text{csch} \frac{\theta_c(n+1)}{2} \text{csch} \frac{\theta_h(n+1)}{2} \left[ e^{i\gamma_1(n+1)\omega_h} - e^{(n+1)(\theta_c + i(\gamma_1\omega_c + \gamma_2\omega_h))} \right] e^{-\frac{n}{2}\{\theta_c + \theta_h + 2i[(\gamma_1 + \gamma_2)\omega_h + \gamma_1\omega_c]\}}$$

$$\times \left[ e^{(n+1)(\theta_h + i\gamma_1\omega_h)} - e^{i(n+1)(\gamma_1\omega_c + \gamma_2\omega_h)} \right], \quad B_1 = \left[ e^{i\gamma_1\omega_h} - e^{\theta_c + i(\gamma_1\omega_c + \gamma_2\omega_h)} \right] \left[ e^{(\theta_h + i\omega_h\gamma_1)} - e^{i(\gamma_1\omega_c + \gamma_2\omega_h)} \right].$$

Using the moments and Eq.(7), the TUR yields as  $\mathcal{Q}_{col}^{(1)} \geq 2 - \langle \Sigma_{col}^{(1)} \rangle$ , where  $\langle \Sigma_{col}^{(1)} \rangle$  and  $\mathcal{Q}_{col}^{(1)}$  are the collective entropy

$$C = -k_B\beta^2 \frac{\partial}{\partial\beta}\text{Tr}[H\rho] = k_B\beta^2 \text{var}(H).$$

If the steady state is restricted to the  $j = n/2$  irreducible subspace with Gibbs's distribution in the common eigenbasis of  $\mathcal{J}_z$  and  $J^2$ ,  $|j, m\rangle$  basis, then we get,  $\langle H \rangle = (n\omega/z) \sum_m (m/n)^x e^{-\beta n\omega(m/n)^x}$ , and  $\langle H^2 \rangle = (n^2\omega^2/z) \sum_m (m/n)^{2x} e^{-\beta n\omega(m/n)^x}$ . At large temperatures, that is inverse temperature  $\beta \rightarrow 0$ , the variance simplifies to  $\text{var}(H) = \langle H^2 \rangle - \langle H \rangle^2 = \frac{n^2\omega^2}{(n+1)} \sum_m \left(\frac{m}{n}\right)^{2x} - \frac{n^2\omega^2}{(n+1)^2} \left(\sum_m \left(\frac{m}{n}\right)^x\right)^2$ . For large  $n$  values, the above summation can be replaced with integration by setting  $q = m/n$  giving,  $\text{var}(H) \approx n^2\omega^2 \left[ \int_{-1/2}^{1/2} q^{2x} dq - \left( \int_{-1/2}^{1/2} q^x dq \right)^2 \right]$ . Again the  $\text{var}(H)$  can be reduced to  $n^2 \frac{\omega^2 x^2}{4^x(2x+1)(x+1)^2}$  for even  $x$ , and  $n^2 \frac{\omega^2}{4^x(2x+1)}$  for odd  $x$ . Thus both work and its variance are found to be proportional to  $n^2$  for any value of  $x$ .

## Appendix C: Characteristic function and moments

The joint probability of having certain values of  $W_3$ ,  $Q_h$  and  $W_1$  during one cycle of the Otto engine can be readily calculated using the chain rule for conditional probabilities,  $P(W = W_3 + W_1, Q_h) = P(W_3, Q_h, W_1) = P(W_3|Q_h, W_1)P(Q_h|W_1)P(W_1)$ . It becomes,  $P(W, Q_h) = \sum_{i,j,m,n} \delta(W - (\epsilon_j^0 - \epsilon_i^r + \epsilon_m^r - \epsilon_n^0)) \delta(Q_h - (\epsilon_i^r - \epsilon_m^r)) p_{n \rightarrow m}^r p_{i \rightarrow j}^r e^{-\beta\epsilon_n^0} e^{-\beta\epsilon_i^r} / (z_\tau z_0)$ . Now the characteristic function,  $\chi$ , can be found by taking the Fourier transform of the  $P(W, Q_h)$ , that is,  $\chi(\gamma_1, \gamma_2) = \iint_{-\infty}^{\infty} dW dQ_h e^{i\gamma_1 W} e^{i\gamma_2 Q_h} P(W, Q_h)$ . It is straightforward to see that the moments can be obtained from the  $\chi$  as [22, 65]  $\langle W^r Q_h^s \rangle = \frac{\partial^r}{\partial(i\gamma_1)^r} \frac{\partial^s}{\partial(i\gamma_2)^s} \chi(\gamma_1, \gamma_2) \Big|_{\gamma_{1,2}=0}$ .

## Collective $n$ spin- $s$ system

For an engine made of  $n$  spin  $s$  systems with  $H = \omega\mathcal{J}_z$ , the characteristic function can be expressed as,  $\chi = A/B$ , where,



production and the quantity  $\mathcal{Q} = \text{var}(W)\langle\Sigma\rangle/\langle W\rangle^2$  for  $x = 1$ . For an  $n$ -independent qubit engine, the TUR reduces to a single qubit TUR,  $\mathcal{Q} \geq 2 - \langle\Sigma\rangle$ , where  $\mathcal{Q}$  and  $\langle\Sigma\rangle$  are respective single qubit quantities.

#### Appendix D: Work fluctuations:

The output work fluctuations of a friction-less Otto engine originate from the thermal energy fluctuations at the two thermalization strokes. Since the energy fluctuations are related to the heat capacity as  $\sigma_E^2 = C/(k_B\beta^2)$ , one would expect the work fluctuations to be equal to the sum of the energy fluctuations at the two thermal strokes. We can show that this is indeed true for a general Hamiltonian  $H = n\omega(\mathcal{J}_z/n)^x$  if the density matrix is given by

an appropriate Gibbs's distribution in  $j = ns$  subspace, and the variance of the work takes the form,  $\text{var}(W) = (\omega_c - \omega_h)^2 \left\{ \frac{C(\theta_h)}{k_B\theta_h^2} + \frac{C(\theta_c)}{k_B\theta_c^2} \right\} \approx \frac{2(\beta_c - \beta_h)^2}{k_B\beta_c^2\beta_h^2} C(\theta_h) + O(\Delta\eta)$ . The above equation holds for both the collective and the independent coupling to the thermal baths for any arbitrary  $x$  values. Again for arbitrary values of  $x$ , it can be shown that  $C(\theta_h) \propto n^2$ .

#### Appendix E: Lower bound on the function $f$

Putting  $\theta_c = \theta_h + \Delta$  in the function  $f(\theta_c, \theta_h) = (\theta_c - \theta_h)(a/b)$  given in Eq. (7) gives  $f(\Delta, \theta_h) = \frac{\Delta[3 - \cosh \Delta - \cosh(\Delta + \theta_h) - \cosh \theta_h]}{\sinh \Delta - \sinh(\Delta + \theta_h) + \sinh \theta_h}$ . In the large  $\theta_h$  limit this becomes,  $f(\Delta) = \Delta \coth \Delta/2 \geq 2$ . Furthermore, a simple numerical analysis yields minima as 2.